We are IntechOpen,
the world's leading publisher of
Open Access books
Built by scientists, for scientists

**4,800**
Open access books available

**122,000**
International authors and editors

**135M**
Downloads

Our authors are among the

**154**
Countries delivered to

**TOP 1%**
most cited scientists

**12.2%**
Contributors from top 500 universities

BOOK CITATION INDEX
CLARIVATE ANALYTICS
INDEXED

**WEB OF SCIENCE**™

Selection of our books indexed in the Book Citation Index
in Web of Science™ Core Collection (BKCI)

Interested in publishing with us?
Contact book.department@intechopen.com

Numbers displayed above are based on latest data collected.
For more information visit www.intechopen.com

**1**

# The Comparative Assessment of Modelling and Control of Mechanical Manipulator

M. H. Korayem, H. N. Rahimi and A. Nikoobin
*Robotic Research Lab, College of Mechanical Engineering,*
*Iran University of Science and Technology*
*Iran*

## 1. Introduction

### 1.1 Overview

In this book chapter a comparative assessment of modelling and control of mechanical manipulator is considered. First, kinematic and dynamic modelling of wide range of mechanical manipulators comprising flexible link, flexible joint and mobile manipulators are considered. Then, open-loop optimal control problem is formulated to control of the obtained system. Finally, some applications of method including motion planning and maximum payload determination are illustrated through the computer simulations.

### 1.2 Problem statement

Mechanical flexibilities can be classified into two categories: Link flexibility and joint flexibility. Link flexibility is a result of applying lightweight structure in manipulator arms designed to increase the productivity by fast motion and to complete a motion with small energy requirement. Joint flexibility arises from elastic behavior of the drive transmission systems such as transmission belts, gears and shafts. Mobile manipulators are combined systems consists of a robotic manipulator mounted on a mobile platform. Such systems are able to accomplish complicated tasks in large workspaces. In particular the greatest disadvantage of mobile robotic manipulators is that most of these systems are powered on board with limited capacity. Hence, incorporating light links can minimize the inertia and gravity effects on links and actuators and it results to decrease the energy consumption in the same motion. Hence, lightweight systems have primary importance in design and manufacturing stages of mobile manipulators.

### 1.3 Motivation

Unfortunately, reviewing of the recent literature on modelling and optimization of flexible and mobile manipulators shows that a very scant attention has been paid to study of model that describes both link and joint flexibility, particularly for mobile manipulators. The main motivation for this study is to present a comprehensive modelling and optimal control of flexible link-joint mechanical mobile manipulators. It can provide an inclusive reference for other researchers with comparative assessment view in the future studies.

## 1.4 Prior work

Analyzing of nonlinear dynamic motion of elastic manipulators is a very complex task that plays a crucial role in design and application of such robots in task space. This complexity arises from very lengthy, fluctuating and highly nonlinear and coupled set of dynamic equations due to the flexible nature of both links and joints. The original dynamics of robotic manipulators with elastic arms, being described by nonlinear coupled partial differential equations. They are continuous nonlinear dynamical systems distinguished by an infinite number of degrees of freedom. The exact solution of such systems does not exist. However, most commonly the dynamic equations are truncated to some finite dimensional models with either the assumed modes method (AMM) or the finite element method (FEM).

The assumed mode expansion method was used to derive the dynamic equation of the flexible manipulator (Sasiadek & Green, 2004). Dynamic modelling technique for a manipulator with multiple flexible links and flexible joints was presented based on a combined Euler–Lagrange formulation and assumed modes method (Subudhi & Morris, 2002). Then, control of such system was carried out by formulating a singularly perturbed model and using it to design a reduced-order controller. Combined Euler–Lagrange formulation and assumed modes method was used for driving the equation of motions of flexible mobile manipulators with considering the simply support mode shape and one mode per link (Korayem & Rahimi Nohooji, 2008). Then, open-loop optimal control method was proposed to trajectory optimization of flexible link mobile manipulator for a given two-end-point task in point-to-point motion.

In finite element method, the elastic deformations are analyzed by assuming a known rigid body motion and later superposing the elastic deformation with the rigid body motion (Usoro et al. 1986). One of the main advantages of FEM over the most of other approximate solution methods to modelling the flexible links is the fact that in FEM the connection are supposed to be clamp-free with minimum two mode shapes per each link (Korayem et al. 2009(a)). This ensures to achieve the results that display the nonlinearity of the system properly.

The Timoshenko beam theory and the finite element method was employed to drive the dynamic equation of flexible link planar cooperative manipulators in absolute coordinates (Zhang & Yu, 2004). Dynamic model of a single-link flexible manipulator was derived using FEM and then studied the feed-forward control strategies for controlling the vibration (Mohamed & Tokhi, 2004). Finite element method was used for describing the dynamics of the system and computed the maximum payload of kinematically redundant flexible manipulators (Yue et al., 2001). Then, the problem was formulated for finding the optimal trajectory and maximum dynamic payload for a given point-to-point task. Finally, numerically simulation was carried out for a planar flexible robot manipulator to validate the research work.

The review of the recent literature shows that extensive research has been addressed the elastic joints robotic arms (Korayem et al. 2009(b)). However, there is only limited research works have been reported on a comprehensive model that describes both link and joint elasticity (Rahimi et al. 2009). Moreover, in almost all cases, linearized models of the link flexibility are considered which reduced the complexity of the model based controller (Chen, 2001).

Mobile manipulators have recently received considerable attention with wide range of applications mainly due to their extended workspace and their ability to reach targets that are initially outside of the manipulator reach. A comprehensive literature survey on mobile manipulator systems can be found (Bloch, 2003). A host of issues related to mobile manipulators have been studied in the past two decade. These include for example: dynamic and static stability (Papadopoulos & Rey, 1996), force development and application (Papadopoulos & Gonthier, 1999), maximum payload determination (Korayem & Ghariblu, 2004). However, a vast number of research publications that deal with the mobile manipulators focus on techniques for trajectory planning of such robots (Korayem & Rahimi Nohooji, 2008).

Motion planning for mobile manipulators is concerned with obtaining open-loop or close-loop controls. It steers a platform and its accompanying manipulator from an initial state to a final one, without violating the nonholonomic constraints (Sheng & Qun, 2006). In most studies of trajectory planning for mobile manipulators the end effector trajectory is specified and the optimal motion planning of the base is considered (Mohri et al., 2001), or integrated motion planning of the base and the end effector is carried out (Papadopoulos, et al., 2002). However, because of designing limitation or environmental obstacle in majority of practical application of mobile manipulators especially in repetitive applications, the platform must follow a specified pose trajectory. In this case, designer must control the joint motions to achieve the best dynamic coordination that optimize the defined cost function such as energy consumption, actuating torques, traveling time or bounding the velocity magnitudes. Applications for such systems abound in mining, construction or in industrial factories.

Optimal control problems can be solved with direct and indirect techniques. In the direct method at first the control and state variables are discretized and the optimal control problem is transcribed into a large, constrained and often sparse nonlinear programming problem, then, the resulting nonlinear programming problem is treated by standard algorithm like interior point methods (Wachter & Biegler, 2006). Famous realizations of direct methods are direct shooting methods (Bock & Plitt, 1984) or direct collocation methods (Hargraves & Paris, 1987). However, direct methods are not yield to exact results. They are exhaustively time consuming and quite inefficient due to the large number of parameters involved. Consequently, when the solution of highly complex problems such as the structural analysis of optimal control problems in robotics is required, the indirect method is a more suitable candidate. This method is widely used as an accurate and powerful tool in analyzing of the nonlinear systems. The indirect method is characterized by a "first optimize, then discretize" strategy. Hence, the problem of optimal control is first transformed into a piecewise defined multipoint boundary value problem, which contains the full mathematical information about the respective optimal control problem. In the following step, this boundary value problem is discretized to achieve the numerical solution (Sentinella & Casalino, 2006). It is well known that this technique is conceptually fertile, and has given rise to far-reaching mathematical developments in the wide ranges of optimal dynamic motion planning problems. For example, it is employed in the path planning of flexible manipulators (Rahimi et.al, 2009), for the actuated kinematic chains (Bessonnet & Chessé, 2005) and for a large multibody system (Bertolazzi et al., 2005). A survey on this method is found in (Callies & Rentrop, 2008).

### 1.5 Layout

The balance of the remaining of the chapter is organized as follows. Section 2 provides background information about kinematic and dynamic analysis of the flexible mobile robotic manipulators. Hence, assumed mode and finite element methods are introduced and formulated to dynamic modelling of flexible link manipulators. Then, the flexible model is completed by adding the joint flexibility. After that, formulation is extended to comprise the mobile manipulators. Section 3 consists of a brief review of converting the problem from optimal control to optimization procedure with implementing of Pontryagin's minimum principle. some application examples with the two links flexible mobile manipulator is detailed in this section. Finally, the concluding remarks with a brief summary of the chapter is presented in the last section.

## 2. System modelling

### 2.1 Kinematic analysis

A mobile manipulator consisting of differentially driven vehicle with n flexible links and n flexible revolute joints is expressed in this section (Fig. 1). The links are cascaded in a serial fashion and are actuated by rotors and hubs with individual motors. The flexible joints are dynamically simplified as a linear torsional springs that works as a connector between the rotors and the links. A concentrated payload of mass $m_p$ is connected to the distal link.
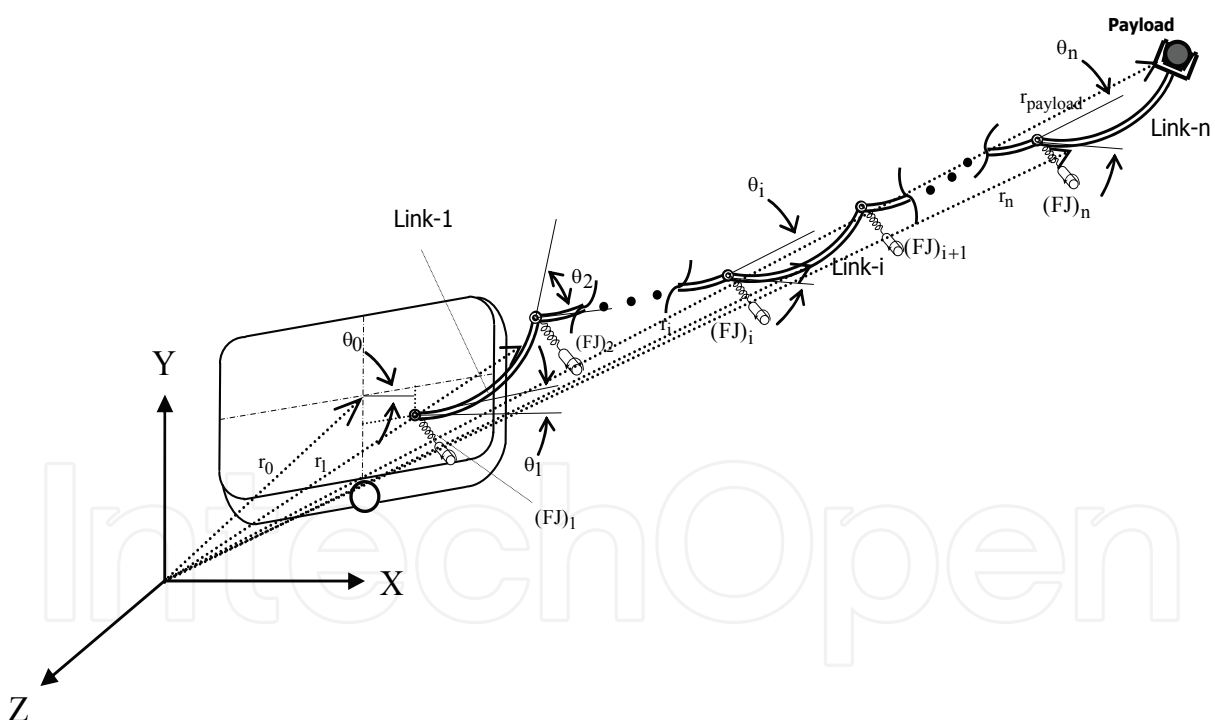


Fig. 1. A schematic view of a multiple flexible links – joints mobile manipulator

The following assumptions are made for the development of a dynamic model of the system.

- Each link is assumed to be long and slender.
- The motion of each link and its deformation is supposed to be in the horizontal plane.
- Links are considered to have constant cross-sectional area and uniform material properties.

- The inertia of payload is neglected.
- The backlash in the reduction gear and coulomb friction effects are neglected.
- It is assumed that the mobile base does not slide.

The generalized coordinates of the flexible links/joints mobile manipulator consist of four parts, the generalized coordinates defining the mobile base motion $\vec{q}_b = (q_{b1}, q_{b2}, \ldots, q_{bn_b})^T$, the generalized coordinates of the rigid body motion of links $\vec{q}_r = (q_1, q_2, \ldots, q_n)^T$ and the generalized coordinates that related to the flexibility of the links $\vec{q}_f = (q_{11}, q_{12}, \ldots, q_{1n_f}, q_{21}, \ldots, q_{2n_f}, \ldots, q_{n1}, \ldots, q_{nn_f})^T$, and the generalized coordinate corresponding to the flexibility of joints $\vec{q}_j = (q_{1+n}, q_{2+n}, \ldots, q_{n+n})^T$. Where n, $n_b$ and $n_f$ are number of links, base degrees of freedom and manipulator mode shapes, respectively.

The notion of redundancy expresses that the number of generalized coordinates (v) is strictly greater than the (global) degree of freedom (d). Thus, the mechanical system is redundant if d<v; and the order of redundancy is v-d. Hence, it is comprehensible that in most mobile manipulator systems $v = n + n_b$ is greater than the end effector degree of freedom in the work space (d). Accordingly, these systems usually are subjected to some non-integrable kinematic constraints known as non-holonomic constraints. There are different techniques, which can be applied to a robotic system to solve the redundancy resolution. Some of these techniques are based on an optimization criterion such as overall torque minimization, minimum joint motion and so on. Hence, Seraji has used r additional user-defined kinematic constraint equations as a function of the motion variables (Seraji, 1998). This method results in a simple and online coordination of the control of a mobile manipulator during motion. The presenting study follows this method. Hence, some additional suitable kinematic constraint equations to the system dynamics are applied. Results are in simple and on-line coordination of the mobile manipulator during the motion. These constraints undertake the robot movement only in the direction normal to the axis of the driving wheels along with previously specification of the base trajectory during the motion.

## 2.2 Dynamic modelling
### 2.2.1 Dynamic modelling of flexible link manipulator

The original dynamics of robotic manipulators with elastic arms, being described by nonlinear coupled partial differential equations. They are continuous nonlinear dynamical systems distinguished by an infinite number of degrees of freedom. The exact solution of such systems does not exist. However, most commonly the dynamic equations are truncated to some finite dimensional models with either the assumed modes method (AMM) or the finite element method (FEM).

2.2.1.1 Assumed mode method

A large number of researchers use assumed modes of vibration to model robot dynamic in order to capture the interaction between flexural vibrations and nonlinear dynamics. In the assumed modes method, the dynamic model of the robot manipulator is described by a set of vibration modes other than its natural modes. Using assumed modes to model flexibility requires Euler–Bernoulli beam theory boundary conditions and accommodates changes in configuration during operation, whereas natural modes must be continually recomputed.

According to this method an approximate deflection of any continuous elastic beam subjected to transverse vibrations, can be expressed through truncated modal expansion, under the planar small deflection assumption of the link as

$$v_i(x_i, t) = \sum_{j=1}^{n_i} \varphi_{ij}(x_i)e_{ij}(t) \qquad i = 1, \ldots, n \tag{1}$$

where $v_i(x_i, t)$ is the bending deflection of the $i^{th}$ link at a spatial point $x_i (0 \leq x_i \leq L_i)$ and $L_i$ is the length of the $i^{th}$ link. $n_i$ is the number of modes used to describe the deflection of link i; $\varphi_{ij}(x_i)$ and $e_{ij}(t)$ are the $j^{th}$ assumed mode shape function and $j^{th}$ modal displacement for the $i^{th}$ link, respectively. Position and velocity of each point on link i can be obtained with respect to inertial coordinate frame using the transformation matrices between the rigid and flexible coordinate systems.

In the AMM there are numerous ways to choose the boundary conditions. The presenting study addresses four well-known conditions and chooses them with one mode shape per each link in the numerical simulations.

Ideally, the optimum set of assumed modes is that closest to natural modes of the system. Hence, there is no stipulation as to which set of assumed modes should be used. Natural modes depend on several factors such as size of hub inertia and size of payload mass. Choosing appropriate conditions is very important and it may cause better consequences in the results. Hence, the ultimate choice requires an assessment based on the actual robot structure and for example, anticipated range of payloads together with its natural modes.

Firs four normal modes for some familiar mode conditions are described as following:

Clamped-free mode shapes are given by

$$\varphi_i(x_i) = \sin(B_i.x_i) - \sinh(B_i.x_i) + A(\cos(B_i.x_i) - \cosh(B_i.x_i))$$
$$where$$
$$A_i = \frac{\cos(B_i.L_i) + \cosh(B_i.L_i)}{\sin(B_i.L_i) - \sinh(B_i.L_i)} \tag{2}$$
$$B_i.L_i : 1.87 \quad 4.69 \quad 7.85 \quad 10.99..$$

Also, clamped – clamped mode shapes are determined as

$$\varphi_i(x_i) = \sin(B_i.x_i) - \sinh(B_i.x_i) + A(\cos(B_i.x_i) - \cosh(B_i.x_i))$$
$$where$$
$$A_i = \frac{\cos(B_i.L_i) - \cosh(B_i.L_i)}{\sin(B_i.L_i) + \sinh(B_i.L_i)} \tag{3}$$
$$B_i.L_i : 4.73 \quad 7.85 \quad 10.99 \quad 14.13.$$

In addition, mode shape functions with clamped-pinned boundary conditions are given by

$$\varphi_i(x_i) = \sin(B_i.x_i) - \sinh(B_i.x_i) + A(\cos(B_i.x_i) - \cosh(B_i.x_i))$$
$$where$$
$$A_i = -\frac{\sin(B_i.L_i) + \sinh(B_i.L_i)}{\cos(B_i.L_i) + \cosh(B_i.L_i)} \tag{4}$$
$$B_i.L_i : 3.92 \quad 7.06 \quad 10.21 \quad 13.35.$$

Similarly, this theory determines pinned–pinned mode shapes as:

$$\varphi_i(x_i) = A_i \sin(B_i.x_i)$$

$$A_i = \frac{\cosh(B_i.L_i)}{\cos(B_i.L_i)}$$

$$B_i.L_i : 3.14 \quad 6.28 \quad 9.42 \quad 12.56. \tag{5}$$

Choosing the appropriate set of assumed modes as a boundary condition may be quite valuable for robot to fit in a suitable application. Ideally, the optimum set of assumed modes is that closest to natural modes of the system. Natural modes depend on several factors within the robotic system ensemble including size of hub inertia and size of payload mass. For large joint gearing inertia and relatively small payload mass, the link may be considered clamped at the joint. Conversely, for smaller joint gearing inertia and larger payload mass both ends of the link may be considered pinned. The ultimate choice requires an assessment based on the actual robot structure and anticipated range of payloads together with its natural modes.

Although assume mode method has been widely used, there are several ways to choose link boundary conditions and mode eigen-functions. This drawback may increase drastically when finding modes for links with non-regular cross sections and multi-link manipulators is objected. In addition, using the AMM to derive the equations of motion of the flexible manipulators, only the first several modes are usually retained by truncation and the higher modes are neglected.

### 2.2.1.2 Finite element method

The finite element method is broadly used to derive dynamic equations of elastic robotic arms. Researcher usually used the Euler–Bernoulli beam element with multiple nodes and Lagrange shape function to achieve the reasonable finite element model. The node number can be selected according to requirement on precision. But, increasing the node number may enlarge the stiffness matrix and it cause to long and complex equations. Hence, choosing the proper node number is very important in the finite element analyzing.

The overall finite element approach involves treating each link of the manipulator as an assemblage of n elements of length $L_i$. For each of these elements the kinetic energy $T_{ij}$ and potential energy $V_{ij}$, are computed in terms of a selected system of generalized coordinate q and their rate of change $\dot{q}$. Note that subscript ij refer to the $j^{th}$ element of link i.

In summary the kinetic energy $T_{ij}$ and potential energy $V_{ij}$ are computed by the following equation:

$$T_{ij} = \frac{1}{2} \int_0^{l_i} m_i \left[ \frac{\partial r_i^T}{\partial t} \cdot \frac{\partial r_i}{\partial t} \right] dx_{ij} \tag{6}$$

And

$$V_{ij} = V_{gij} + V_{eij}$$

$$= \int_0^{l_i} m_i g \begin{bmatrix} 0 & 1 \end{bmatrix} T_0^1 \begin{bmatrix} (j-1)l_i + x_{ij} \\ y_{ij} \end{bmatrix} dx_{ij} + \frac{1}{2} \int_0^{l_i} EI_i \left[ \frac{\partial^2 y_{ij}}{\partial x_{ij}^2} \right]^2 dx_{ij} \tag{7}$$

In above equation, the potential energy is consisted of two parts. One part is due to gravity ($V_{gij}$) and another is related to elasticity of links ($V_{eij}$). $r_i$, $m_i$, $l_i$ and $EI_i$ are the position, mass, length and the flexural rigidity of $i^{th}$ element respectively. $x_{ij}$ and $y_{ij}$ are specified the distances along body- fixed system $O_{ij}X_{ij}Y_{ij}$ from common junction between elements 'i(j-1)'

and 'ij' of link i. $T_0^1 = \begin{bmatrix} \cos(\theta_1) & -\sin(\theta_1) \\ \cos(\theta_1) & \sin(\theta_1) \end{bmatrix}$ is transformation matrix from body-fixed system attached to link 1 to inertial system of coordinates and $\theta_1$ is it's correlated joint angle. These energies of elements are then combined to obtain the total kinetic energy T, and potential energy V, for the each link. Knowledge of the kinetic and potential energies is tantamount to specify the Lagrangian £ of the system, given by £=T-V. Using of finite element method in modelling of the robotics system are details in (Usoro, 1986).

As it can be seen, modelling of flexural vibrations of robotic elements using finite element is a well-established technique. So, researchers can handle nonlinear conditions with this method. However, in order to solve a large set of differential equations derived by the finite element method, a lot of boundary conditions have to be considered, which are, in most situations, uncertain for flexible manipulators. Also, although significant advantages of FEM over analytical solution techniques such as easy to handle with which nonlinear conditions, this approach seems more complex over AMM. The main reason is that use of the finite element model to approximate flexibility usually gives rise to an overestimated stiffness matrix. Moreover, because of the large number of equations, the numerical simulation time may be exhausting for the finite element models.

2.2.1.3 Numerical simulations

The dynamic equations of the flexible robotic arms are verified in this section by undertaking a computer simulation. Hence, the case of harmonic motion of a nonlinear model of flexible robotic arms is selected to simulation. In this simulation, the robot is hanged freely and it influenced only under gravity effect. The physical parameters of the system used in this simulation study were $L_1 = L_2 = 1\,m$, $I_1 = I_2 = 5 \times 10^{-9}\,m^4$, $m_1 = m_2 = 5\,kg$ and $E_1 = E_2 = 2 \times 10^{11}\,N/m^2$. Simulating both FEM and AMM (pinned-pinned and clamped-pinned) models and comparing them with the rigid links in this simulation shows the oscillatory behavior of nonlinear robotic system advisably.

Now, considering the equations describe in the last section for FEM and AMM, also, using Lagrangian formulation, the set of equation of motion for each method is derived in compact form as

$$M(q)\ddot{q} + H(q, \dot{q}) = U \tag{8}$$

where M is the inertia matrix, H is the vector of Coriolis and centrifugal forces in addition to the gravity effects vector and U is the generalized force vector inserted into the actuator.

Open loop system response of changing the initial condition from normal equilibrium position to the relative angle between the first and second link of this system ($\theta_2$) to the deviation of 5 degree is studied in this simulation (Fig. 2).

The responses of the system are presented in Figs. 3-5. Figures show the difference between rigid and flexible robotic arms also between the FEM and AMM with both pinned- pinned and clamped- pinned boundary conditions.

Figs. 3 and 4 show the angular positions and angular velocities of joints. It is obvious from figures that the link elasticity appears in velocity graph more and more than the position graph. Also, these figures restate the issue that the FEM model displays the nonlinearity of the system properly.

The corresponding amplitudes of vibration modes in the AMM are shown in Fig. 5. It is clear that link flexibility significantly affects the link vibrations. In addition, pictures shows that these effects are appeared more when clamped – pinned boundary condition is

considered. Figures are plotted in this section clearly show a good agreement between the obtained results in this study and those presented in (Usoro, 1986).
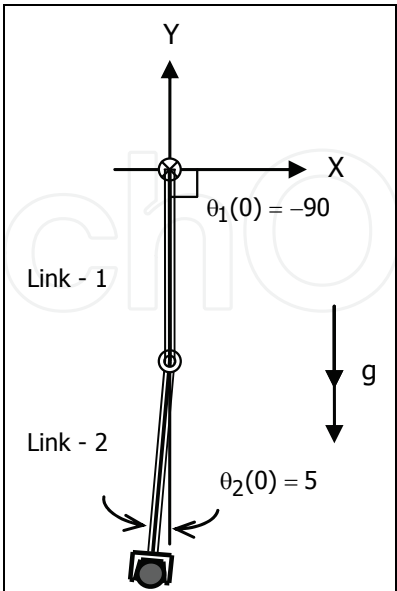


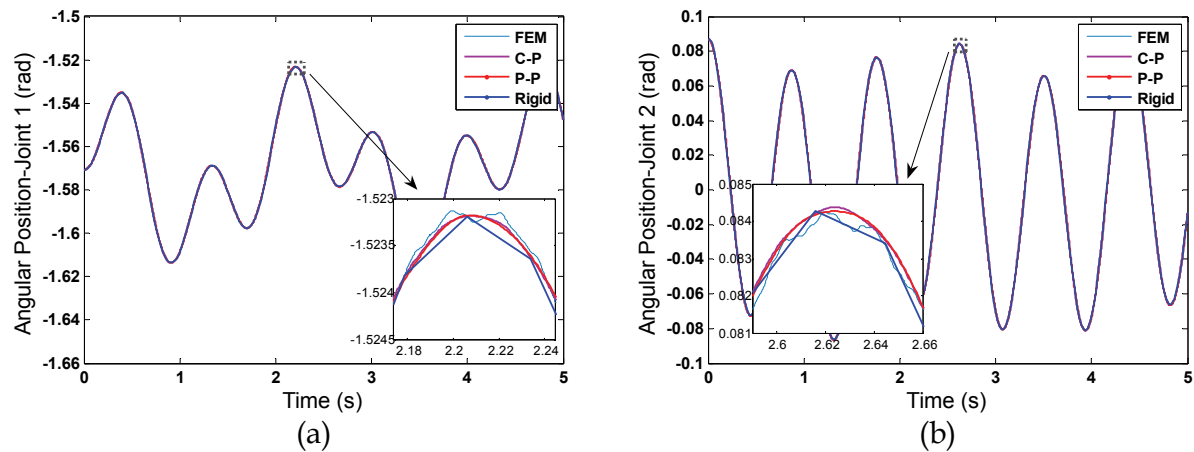Fig. 2. Initial robot configuration



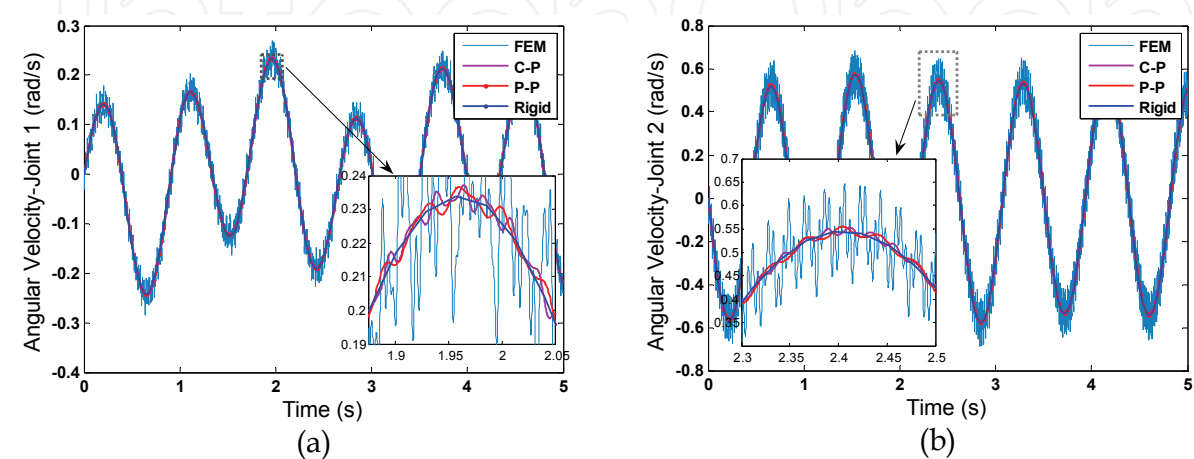Fig. 3. Angular position of joints: (a) joint 1; (b) joint 2.



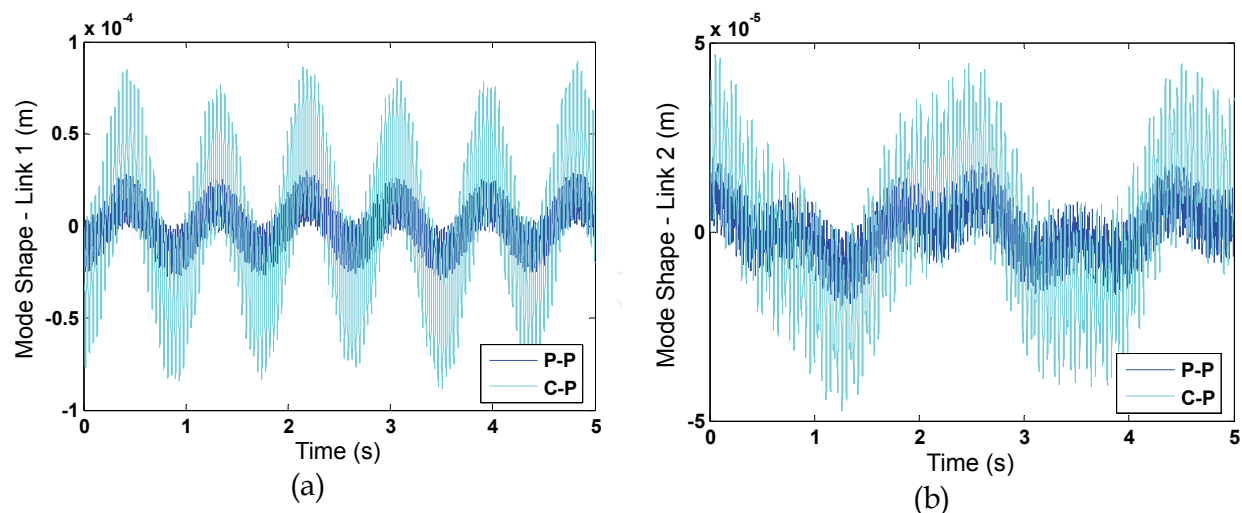Fig. 4. Angular velocity of joints: (a) joint 1; (b) joint 2.

Fig. 5. Amplitudes of vibration's modes: (a) Link 1; (b) Link 2

### 2.2.2 Dynamic modelling of flexible joint manipulator

To model a flexible joint manipulator (FJM) the link positions are let to be in the state vector as is the case with rigid manipulators. Actuator positions must be also considered because in contradiction to rigid robots these are related to the link position through the dynamics of the flexible element. By defining the link number of a flexible joint manipulator is $m$, position of the $i^{th}$ link is shown with $\theta_{2i-1} : i = 1, 2, ..., m$ and the position of the $i^{th}$ actuator with $\theta_{2i} : i = 1, 2, ..., m$, it is usual in the FJM literature to arrange these angles in a vector as follows:

$$Q = \left[ \theta_1, \theta_3, ... \theta_{2m-1} \mid \theta_2, \theta_4, ... \theta_{2m} \right]^T = \left[ q_1^T, q_2^T \right]^T \tag{9}$$

So by adding the joint flexibility with considering the elastic mechanical coupling between the $i^{th}$ joint and link is modeled as a linear torsional spring with constant stiffness coefficient $k_i$, the set of equation of motion comprising mobile base with both link and joint flexibility can be rearranged into the following form:

$$\begin{aligned} M(q_1)\ddot{q}_1 + H(q_1, \dot{q}_1) + G(q_1) + K(q_1 - q_2) = 0 \\ J\ddot{q}_2 + K(q_2 - q_1) = U \end{aligned} \tag{10}$$

where K=diag[ $k_1, k_2, ..., k_m$ ] is a diagonal stiffness matrix which models the joint elasticity, J=diag[ $J_1, J_2, ..., J_m$ ] is the diagonal matrix representing motor inertia.

A simulation is performed to investigate the effect of joint flexibility on the response of model by adding the elasticity at each joint as a linear spring. The case study with clamped-pinned boundary condition is modeled for that issue. Simulation is done at the overall time 5 seconds. Parameter values of joints are $k_1 = k_2 = 1500$ N.m and $J_1 = J_2 = 2$ kg. $m^2$.

As shown in Fig. 6 the joint flexibility has considerable consequences on the robot behavior and link parameters have significant deviations from rotor's one. Hence, it can be conclude that the joint flexibility, considerably influences the performance of robotic arms and it can

be as a significant source of nonlinearity and system's oscillatory behavior. Therefore, it is recommended that to improve the performance of the robotic systems, joint flexibility taken into account in modelling and control of such systems.
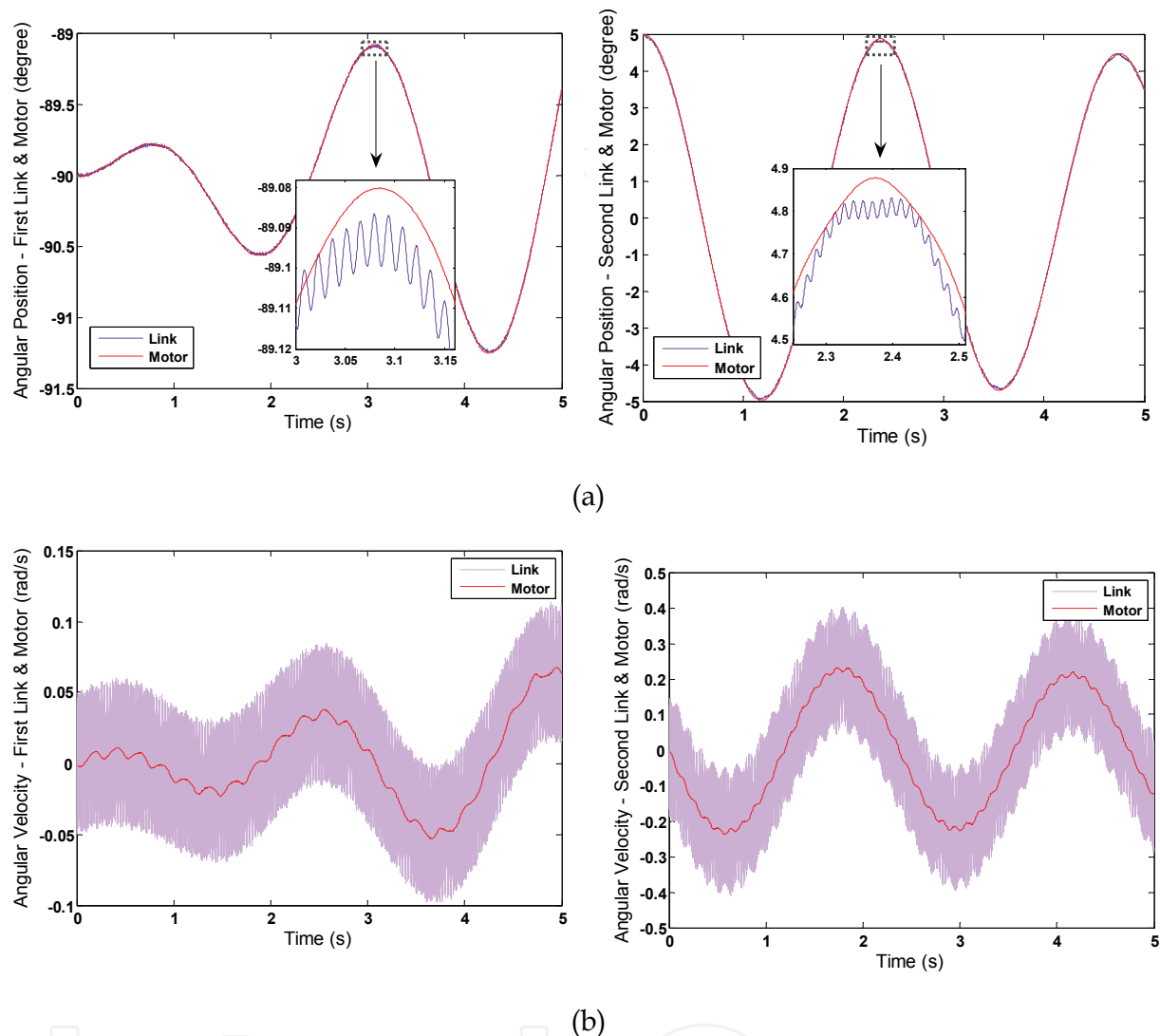


(a)



(b)

Fig. 6. Effect of joint flexibility in (a) Position and (b) Velocity of joints

### 2.2.4 Dynamic modelling of mobile manipulator

Consider an n DOFs rigid mobile manipulator with generalized coordinates $q = [q_i]$, $i = 1, 2, ..., n$ and a task described by m task coordinates $r_j$, $j = 1, 2, ..., m$ with m < n. By applying h holonomic constraints and c non-holonomic constraints to the system, $r = h + c$ redundant DOFs of the system can be directly determined. Therefore m DOFs of the system is remained to accomplish the desired task. As a result, we can decomposed the generalized coordinate vector as $q = \begin{bmatrix} q_r & q_{nr} \end{bmatrix}^T$, where $q_r$ is the redundant generalized coordinate vector determined by applying constraints and $q_{nr}$ is the non-redundant generalized coordinate vector. By considering the flexible link manipulators instead of the rigid ones, their related generalized coordinates, $q_f$, are added to the system; therefore, the overall decomposed generalized coordinate vector of system obtain as $q = \begin{bmatrix} q_r & q_{nrf} \end{bmatrix}^T$, where $q_{nrf}$ is the combination vector of $q_{nr}$ and $q_f$.

The system dynamics can also be decomposed into two parts: one is corresponding to redundant set of variables, $q_r$ and the remained set of them, $q_{nrf}$. That is,

$$\begin{bmatrix} M_{r,r} & M_{r,nrf} \\ M_{r,nrf} & M_{nrf,nrf} \end{bmatrix} \begin{bmatrix} \ddot{q}_r \\ \ddot{q}_{nrf} \end{bmatrix} + \begin{bmatrix} C_r + G_r \\ C_{nrf} + G_{nrf} \end{bmatrix} = \begin{bmatrix} U_r \\ U_{nrf} \end{bmatrix} \tag{11}$$

where by considering the second row in order to path optimization procedure leads to

$$U_{nrf} = A\ddot{q}_{nrf} + B . \tag{12}$$

Using redundancy resolution $q_r$ will be obtained as a known vector in terms of the time (t). Therefore A is obtained as a function of time and $q_{nrf}$ and B as a function of time, $q_r$ and $\dot{q}_{nrf}$.

By defining the state vector as

$$X = \begin{bmatrix} X_1 & X_2 \end{bmatrix}^T = \begin{bmatrix} q_{nrf} & \dot{q}_{nrf} \end{bmatrix}^T , \tag{13}$$

Eq. (5) can be rewritten in state space form as

$$\dot{X} = \begin{bmatrix} \dot{X}_1 \\ \dot{X}_2 \end{bmatrix} = \begin{bmatrix} X_2 \\ N(X) + D(X)U \end{bmatrix} = \begin{bmatrix} F_1 \\ F_2 \end{bmatrix}, \tag{14}$$

where $D = M^{-1}$ and $N = -M^{-1}(C(X_1,X_2) + G(X_1))$. Then, optimal control problem is determined the position and velocity variable $X_1(t)$ and $X_2(t)$, and the joint torque U (t) which optimize a well-defined performance measure when the model is given in Eq. (14).

## 3. Optimal control

### 3.1 Defining the optimal control problem

Pontryagin's minimum principle provides an excellent tool to calculate optimal trajectories by deriving a two-point boundary value problem. Let the trajectory generation problem be defined here as determining a feasible specification of motion, which will cause the robot to move from a given initial state to a given final state. The method presented in this article adapts in a straightforward manner to the generation of such dynamic profiles.

There are known that nonlinear system dynamics stated as Eq. (14) be expressed in the term of states (X), controls (U) and time (t) as

$$\dot{X} = f(X,U,t) \tag{15}$$

Generating optimal movements can be achieved by minimizing a variety of quantities involving directly or not some dynamic capacities of the mechanical system. A functional is considered as the integral

$$J(u) = \int_{t_0}^{t_f} L(X,U,t)dt \tag{16}$$

where the function L may be specified in quite varied manners. There are initial and terminal constraints on the states:

$$X(t_0) = X_0 \qquad X(t_f) = X_f \qquad (17)$$

There may also be certain pragmatic constraints (reflecting such concerns as limited actuator power) on the inputs. For example:

$$|U(t)| \leq U_{\max}(t) \qquad (18)$$

According to the minimum principle of Pontryagin (Kirk, 1970), minimization of performance criterion at Eq. (16), is achieved by minimizing the Hamiltonian (H) which is defined as follow:

$$H(X,U,\Psi,m_p,t) = L(X,U,m_p,t) + \Psi^T f(X,U,t) \qquad (19)$$

where $\Psi(t) = \begin{bmatrix} \psi_1(t)^T & \psi_2(t)^T \end{bmatrix}^T$ is the nonzero costate time vector-function.

Finally, according to the aforementioned principle, stating the costate vector-equation

$$\dot{\Psi}^T = -\partial H / \partial X \qquad (20)$$

in addition to the minimality condition for the Hamiltonian as

$$\partial H / \partial U = 0 \qquad (21)$$

$$\dot{X} = \partial H / \partial \Psi , \qquad (22)$$

leads to transform the problem of optimal control into a non-linear multi-point boundary value problem.

Consequently, for a specified payload value, substituting obtained computed control equations from Eqs. (21) and Eq. (18) into Eqs. (20) and (22), sixteen nonlinear ordinary differential equations are obtained which with sixteen boundary conditions given in Eq. (17), constructs a Two Point Boundary Value Problem(TPBVP). Such a problem is solvable with available commands in different software such as MATLAB and MATEMATHICA.

### 3.2 Application
### 3.2.1 Developing for two-link flexible mobile manipulator

3.2.1.1 Equations of motion

In this section, a mobile manipulator consists of a mobile platform with two flexible links / joints manipulator as depicted in Fig. 7 is considered to analysis. For study on the complete model, first, a mobile manipulator with two flexible links is considered to derive the dynamic equations, then, with applying the joint flexibility by modelling the elasticity at each joint as a linear torsinal spring the model is developed for integrated link and joint flexible mobile manipulator.

To model the equations of motion of the system, assumed mode method is used. For this purpose, the total energy associated with the system must be computed to determine the Lagrangian function.
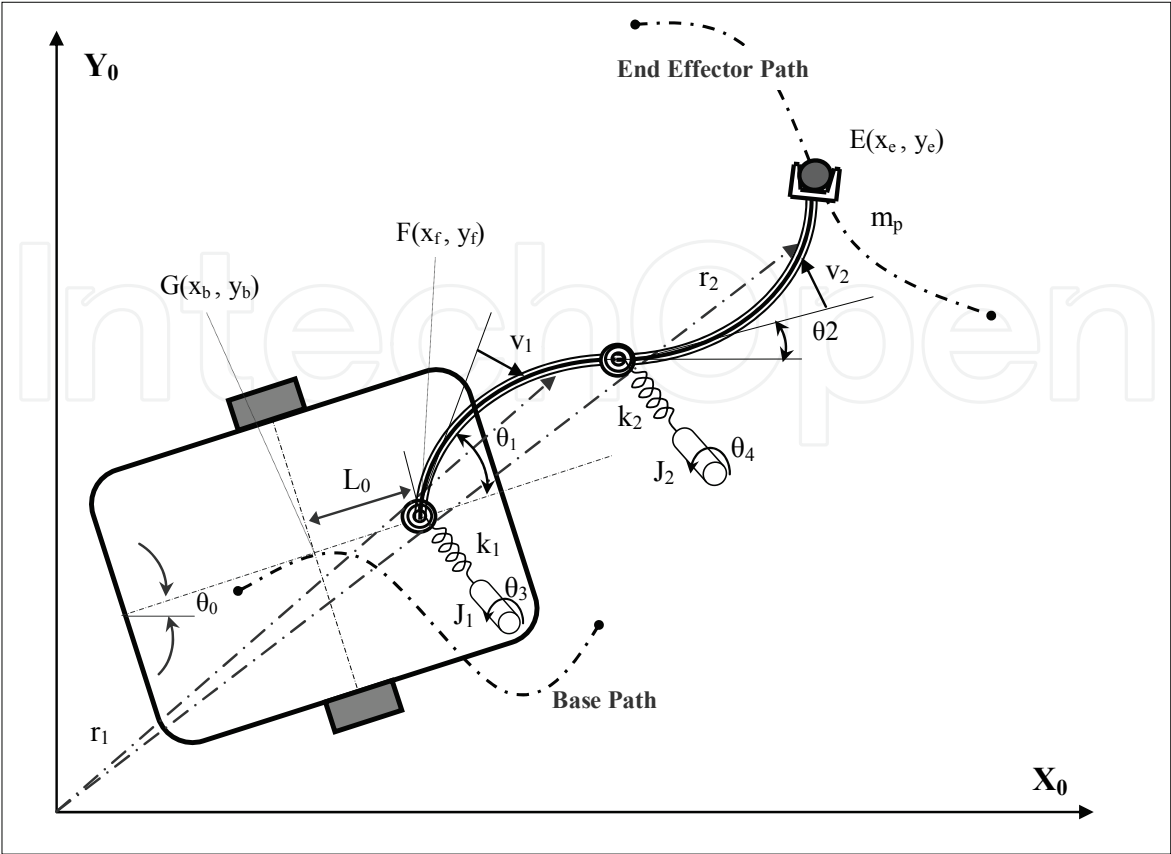
Fig. 7. Two links mobile manipulator with flexible links and joints

The total kinetic energy of the system (T) is given by

$$T = T_L + T_B + T_M ,$$ (23)

The kinetic energy of flexible links can be found as

$$T_L = \sum_{i=1}^{2} \frac{1}{2} \rho_i \int_0^{L_i} \dot{r}_i^T(x_i)\, \dot{r}_i(x_i)\, dx_i ,$$ (24)

where $r_i$ is the position vector that describes an arbitrary point along the $i^{th}$ deflected link with respect to the global co-ordinate frame ($X_0 Y_0$) and $\rho_i$ is the linear mass density for the $i^{th}$ link.

By defining $r_b$ and $r_m$ as position vectors of the base and the payload respectively, the associated kinetic energies are obtained as:

$$T_M = \frac{1}{2} m_p \dot{r}_m^2$$
$$T_B = \frac{1}{2} m_b \dot{r}_b^2 + \frac{1}{2} I_b \dot{\omega}_b^2 ,$$ (25)

where $I_b$ and $\dot{\omega}_b$ are the moment of inertia and the angular velocity of base, respectively. Note that the moment of inertia of the end effector has been neglected.

Next, the potential energy associated with the flexibility of the links due to the link deformation is obtained as:

$$U_L = \sum_{i=1}^{2} \frac{1}{2} \int_0^{L_i} (EI)_i \left( \frac{d^2 v_i}{dx_i^2} \right) dx_i , \tag{26}$$

where $(EI)_i$ is the flexural rigidity of the $i^{th}$ link and $v_i(x_i, t)$ is the bending deflection of the $i^{th}$ link at a point $x_i, (0 \le x_i \le l_i)$. Now, by determining the gravity energy as:

$$U_g = \sum_{i=1}^{2} \int_0^{L_i} \rho_i g x_i dx_i , \tag{27}$$

and adding this energy to those obtained in Eq. (26) the total potential energy of the system is obtained as $U = U_L + U_g$. Finally, by constructing the Lagrangian as L = T – U and using the Lagrangian equation, the equations of motion for two-link flexible mobile manipulator can be obtained as Eq. (8). Hence, the overall generalized co-ordinate vector of the system can be written as: $q = [q_b \quad q_r \quad q_f] = [x_f \quad y_f \quad \theta_0 \quad \theta_1 \quad \theta_2 \quad e_1 \quad e_2]$, where $q_b = [x_f \quad y_f \quad \theta_0]$ is the base generalized coordinates vector, $q_r = [\theta_1 \quad \theta_2]$ is the link angles vector and $q_f = [e_1 \quad e_2]$ is the vector of link modal displacements.

There is one nonholonomic constraint for the mobile base that undertakes the robot movement only in the direction normal to the axis of the driving wheels:

$$\dot{x}_f \sin(\theta_0) - \dot{y}_f \cos(\theta_0) + L_0 \dot{\theta}_0 = 0 . \tag{28}$$

Now, by predefining the base trajectory, the system dynamics can be decomposed into two parts: one is corresponding to redundant set of variables, $q_r$ and the remained set of them, $q_{nrf}$. That is

$$\begin{bmatrix} M_{r,r} & M_{r,nrf} \\ M_{r,nrf} & M_{nrf,nrf} \end{bmatrix} \begin{bmatrix} \ddot{q}_r \\ \ddot{q}_{nrf} \end{bmatrix} + \begin{bmatrix} H_r \\ H_{nrf} \end{bmatrix} = \begin{bmatrix} U_r \\ U_{nrf} \end{bmatrix} , \tag{29}$$

Now, by remaining the second row of above equation, the non-redundant part of system equations is considered to path optimization procedure.

For developing the system to encounter the flexible joints manipulator, adding the actuator positions and their dynamic equations is required. Hence, the set of system dynamic equation is rearranged as explain in Eq. (10). This overall system is clearly established the equations that involve the flexible nature of both links and joints.

$$\begin{cases} \begin{bmatrix} m_{11} & m_{12} & m_{13} & m_{14} \\ & m_{22} & m_{23} & m_{24} \\ & & m_{33} & m_{34} \\ Sym & & & m_{44} \end{bmatrix} \begin{bmatrix} \ddot{\theta}_1 \\ \ddot{\theta}_2 \\ \ddot{e}_1 \\ \ddot{e}_2 \end{bmatrix} + \begin{bmatrix} h_1 \\ h_2 \\ h_3 \\ h_4 \end{bmatrix} + \begin{bmatrix} k_1 & 0 & 0 & 0 \\ 0 & k_2 & 0 & 0 \\ 0 & 0 & 0 & 0 \\ 0 & 0 & 0 & 0 \end{bmatrix} \begin{bmatrix} \theta_1 - \theta_3 \\ \theta_2 - \theta_4 \\ 0 \\ 0 \end{bmatrix} = 0 \\ \begin{bmatrix} J_1 & 0 \\ 0 & J_2 \end{bmatrix} \begin{bmatrix} \ddot{\theta}_3 \\ \ddot{\theta}_4 \end{bmatrix} + \begin{bmatrix} k_1 & 0 \\ 0 & k_2 \end{bmatrix} \begin{bmatrix} \theta_3 - \theta_1 \\ \theta_4 - \theta_2 \end{bmatrix} = \begin{bmatrix} u_1 \\ u_2 \end{bmatrix} \end{cases} \tag{30}$$

These enhanced dynamic equations that involve dynamic of the two-link flexible mobile manipulator are considered in trajectory planning problem in the presenting study.

3.2.1.2 Stating an optimal control solution

Optimal control approach provides an excellent tool to calculate optimal trajectory with high accuracy for robots that include, in this case, two link flexible mobile manipulators.
Let the trajectory generation problem be defined here as determining a feasible specification of motion which will cause the robot to move from a given initial posture (state) to a given final posture (state) while minimize a performance criterion such as integral quadratic norm of actuating torques or velocities, which leads to minimize energy consumption or bounding the velocity magnitude.
For this reason, as it can be seen in Fig. 7 the state vectors can be defined as:

$$X_1 = \begin{bmatrix} \theta_1(t) \\ \theta_2(t) \end{bmatrix} = \begin{bmatrix} x_1(t) \\ x_3(t) \end{bmatrix} \quad X_2 = \begin{bmatrix} \dot{\theta}_1(t) \\ \dot{\theta}_2(t) \end{bmatrix} = \begin{bmatrix} x_2(t) \\ x_4(t) \end{bmatrix}$$

$$X_3 = \begin{bmatrix} e_1(t) \\ e_2(t) \end{bmatrix} = \begin{bmatrix} x_5(t) \\ x_7(t) \end{bmatrix} \quad X_4 = \begin{bmatrix} \dot{e}_1(t) \\ \dot{e}_2(t) \end{bmatrix} = \begin{bmatrix} x_6(t) \\ x_8(t) \end{bmatrix} \tag{31}$$

$$X_5 = \begin{bmatrix} \theta_3(t) \\ \theta_4(t) \end{bmatrix} = \begin{bmatrix} x_9(t) \\ x_{11}(t) \end{bmatrix} \quad X_6 = \begin{bmatrix} \dot{\theta}_3(t) \\ \dot{\theta}_4(t) \end{bmatrix} = \begin{bmatrix} x_{10}(t) \\ x_{12}(t) \end{bmatrix}.$$

where $\theta_1$ and $\theta_2$ are angular positions of links, $e_1$ and $e_2$ are links modal displacements, and $\theta_3$ and $\theta_4$ are angular positions of motors. The boundary condition can be expressed as:

$$x_1(0) = x_9(0) = x_{10}, \quad x_3(0) = x_{11}(0) = X_{30};$$
$$x_1(f) = x_9(f) = X_{1f}, \quad x_3(f) = x_{11}(f) = X_{3f}; \tag{32}$$

Other boundary conditions are assumed to be zero.
Now, with defining $Z_{4\times4} = M_{4\times4}^{-1}$ and $I_{2\times2} = J_{2\times2}^{-1}$ Eq. (30) can be rewritten in the compact form as:

$$\ddot{q}_1 = Z(K(q_{21} - q_{11}) - H) = F_1$$
$$\ddot{q}_2 = I(U - K(q_{22} - q_{12})) = F_2, \tag{33}$$

where $q_{21} = (x_1 \quad x_3 \quad 0 \quad 0)$, $q_{11} = (x_9 \quad x_{11} \quad 0 \quad 0)$, $q_{22} = (x_1 \quad x_3)$, $q_{12} = (x_9 \quad x_{11})$, and $U = (u_1 \quad u_2)$. Remember that in this simulation the gravity effect is assumed to be zero.
Hence, by defining the vector F as: $F = [F_1 \quad F_2] = [f_1 \quad f_2 \quad f_3 \quad f_4 \quad f_5 \quad f_6]$ the set of state space equations of system can be written as:

$$\dot{x}_{2i-1} = x_{2i} ;$$
$$\dot{x}_{2i} = f_i \quad ; \quad i = 1...6 \tag{34}$$

In order to derive the equations associated with optimality conditions, penalty matrices can be selected as follows:

$$W = diag(w_1, w_2, w_3, w_4, w_5, w_6)$$
$$R = diag(r_1, r_2). \tag{35}$$

An important remark must be done here is that the study is planned a trajectory in the joint space rather than in the operating space. It means the control system acts on the manipulator joints rather than on the end effector. Trajectory planning in the joint space would allow avoiding the problems arising with kinematic singularities and manipulator redundancy. Moreover, it would be easier to adjust the trajectory according to the design requirements if working in the joint space. By controlling manipulator joints can achieve the best dynamic coordination of joint motions, while minimizing the actuating inputs together with bounding the velocity magnitudes. It causes to ensure soft and efficient functioning while improving the manipulator working performances. For that reason, the objective function is formed as:

$$L = \frac{1}{2}\left(r_1 u_1^2 + r_2 u_2^2 + \sum_{i=1}^{6} w_i x_{2i}^2\right). \tag{36}$$

Subsequently, with defining the auxiliary costate vector as: $\Psi = \begin{bmatrix} \psi_1 & \psi_2 & \dots & \psi_{12} \end{bmatrix} = \begin{bmatrix} x_{13} & x_{14} & \dots & x_{24} \end{bmatrix}$ results to the Hamiltonian function as:

$$H = \frac{1}{2}\left(r_1 u_1^2 + r_2 u_2^2 + \sum_{i=1}^{6} w_i x_{2i}^2\right) + \sum_{i=1}^{12} x_{12+i}\dot{x}_i, \tag{37}$$

Consequently, with differentiating the Hamiltonian function with respect to states, the costate equations are obtained as follow

$$\dot{\psi}_i = -\frac{\partial H}{\partial x_i}, \ i = 1, \cdots, 12. \tag{38}$$

Also, differentiating the Hamiltonian with respect to control and setting the derivative equal to zero, yields the following control equations:

$$\frac{\partial H}{\partial u_1} = r_1 u_1 + x_{23}/J_1 = 0 \quad ; \quad \frac{\partial H}{\partial u_1} = r_2 u_2 + x_{24}/J_2 = 0 \tag{39}$$

where by solving them, the expression for control values in the admissible interval, $u_i^- < u_i < u_i^+ \ ; \ i = 1, 2$ can be obtained as follow:

$$u_1 = -x_{23}/(r_1 J_1) \quad ; \quad u_2 = -x_{24}/(r_2 J_2). \tag{40}$$

Then, by considering the constraint on control input, the optimal control can be expressed as follows:

$$u_1 = \begin{cases} u_1^+ & -x_{23}/(r_1 J_1) \geq u_1^+ \\ -x_{23}/(r_1 J_1) & otherwise \\ u_1^- & -x_{23}/(r_1 J_1) \leq u_1^- \end{cases}$$

$$\tag{41}$$

$$u_2 = \begin{cases} u_2^+ & -x_{24}/(r_2 J_2) \geq u_2^+ \\ -x_{24}/(r_2 J_2) & otherwise \\ u_2^- & -x_{24}/(r_2 J_2) \leq u_2^- \end{cases}$$

where the final bound of control for each motor is obtained as:

$$
\begin{aligned}
u_1^+ &= \tau_1 - S_1\, x_{11} \quad ; \quad u_1^- = -\tau_1 - S_1\, x_{11} \\
u_2^+ &= \tau_2 - S_2\, x_{12} \quad ; \quad u_2^- = -\tau_2 - S_2\, x_{12}
\end{aligned}
\tag{42}
$$

where $S_i = (\tau_i / \omega_{mi})$, $\tau_i$ and $\omega_{mi}$ are the stall torque and maximum no-load speed of $i^{th}$ motor respectively.

Finally, 24 nonlinear ordinary differential equations are obtained by substituting Eq.(33) into Eqs. (38) and (34), which with 24 boundary conditions given in Eq.(32) construct a two point boundary value problem (TPBVP).

There are numerous influential and efficient commands for solving such problems that are available in different software such as MATLAB, MATEMATHICA or FORTRAN. These commands by employing capable methods such as finite difference, collocation and shooting method solve the problem. In this study, BVP4C command in MATLAB® which is based on the collocation method is used to solve the aforesaid problem. This numerical technique have been detailed by (Shampine et al.).

3.2.1.3 Required parameters

In all simulations the mobile base is initially at point ($x_{fi}$ = 0.5m, $y_{fi}$ = 0.5m, $\theta_{fi}$ = 0) and moves along a straight-line path to final position ($x_{ff}$ = 1.5m, $y_{ff}$ = 1m). The necessary parameters used in the simulations are summarized in the Table 1.

| Properties | Symbol | Value (Unit) |
|---|---|---|
| Length of Links | l | 1(m) |
| Mass Density | $\rho$ | 6 (kg. m$^{-1}$) |
| Flexural Rigidity | EI | 100 ( N.m$^2$ ) |
| Max. no Load Speed of Actuators | $\omega_s$ | 6 (rad / s) |
| Actuator Stall Torque | $\tau_s$ | 25 (N. m) |
| Moment of Inertia (Motor) | J | 2 (kg. m$^2$ ) |
| Spring Constant | k | 1000 Nm |

Table 1. System parameters

Velocity at start and stop is considered to be zero. Other boundary conditions are assumed to be:

$$
\begin{aligned}
x_1(0) &= x_9(0) = 120^\circ, \quad x_3(0) = x_{11}(0) = 90^\circ; \\
x_1(f) &= x_9(f) = 30^\circ, \quad x_3(f) = x_{11}(f) = 30^\circ;
\end{aligned}
\tag{43}
$$

Also, in all simulations, the penalty matrix of control efforts R assumes to be R=diag[0.01]. Note that in all simulations, the payload is calculated with the accuracy of 0.1 Kg.

## 3.2.2 Motion planning

3.2.2.1 Motion planning for different penalty matrixes

In the first case, effects of changing in performance index in the path planning problem are investigated. Hence, simulation is done for the different values of W and optimal paths for a given payload are obtained.

By considering penalty matrices as W = (w, w, 0, 0, w, w) by zero the first path is determined. Other paths are drowning with scaling up the value of W as: 1, 100, and 1000. Note that in these simulations the penalty matrices refer to velocities of mode shapes are fixed in zero and the payload is assumed to be 1 Kg.
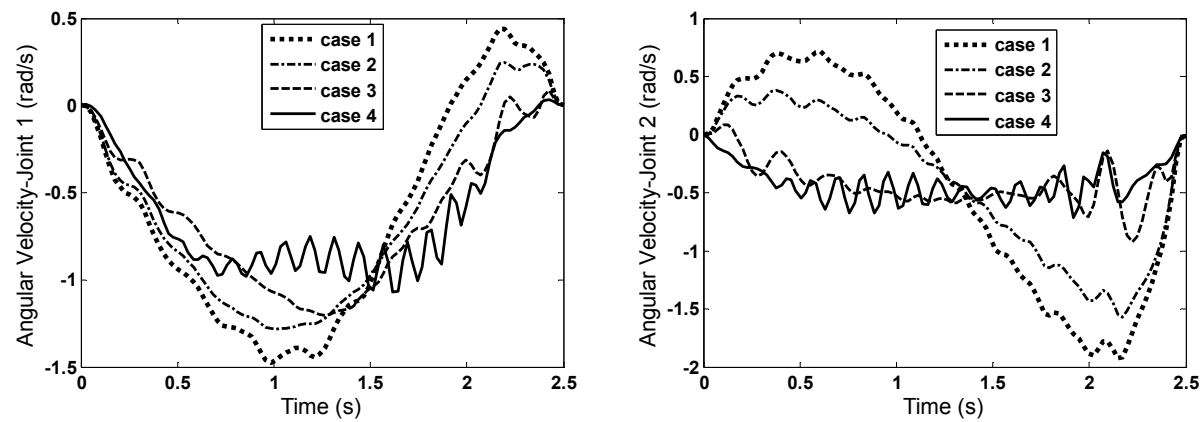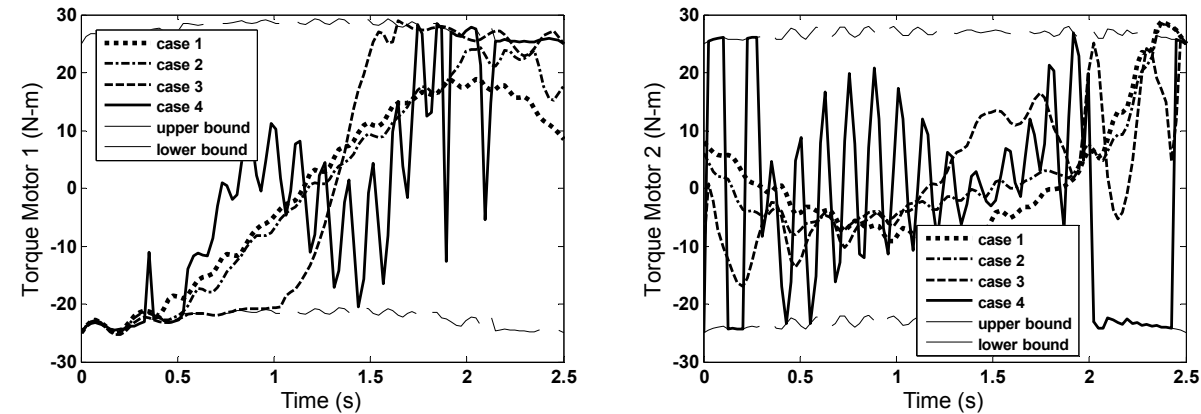


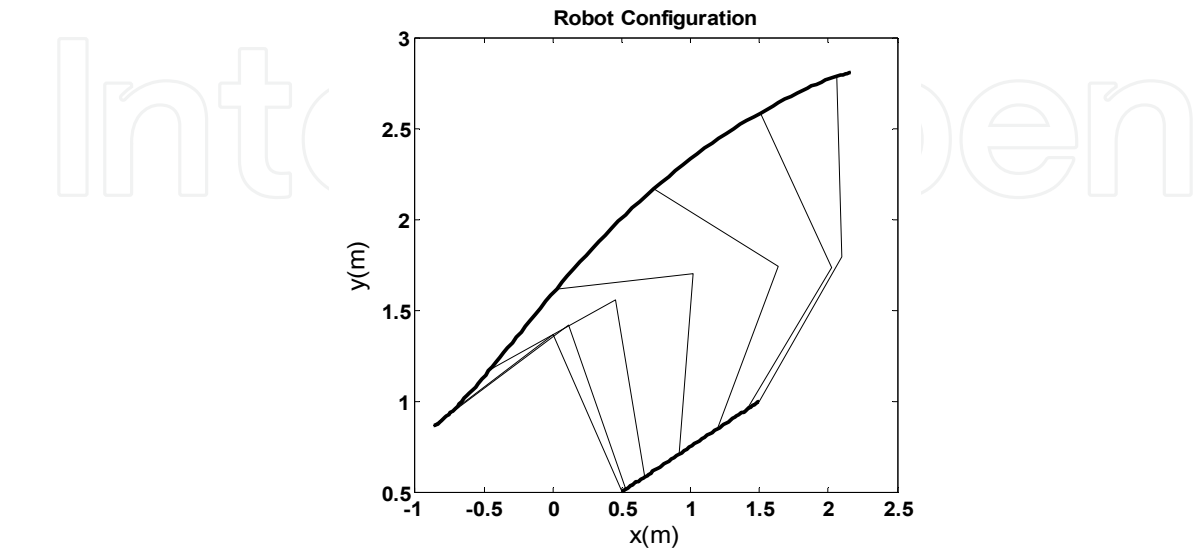Fig. 8. Angular velocities of joints



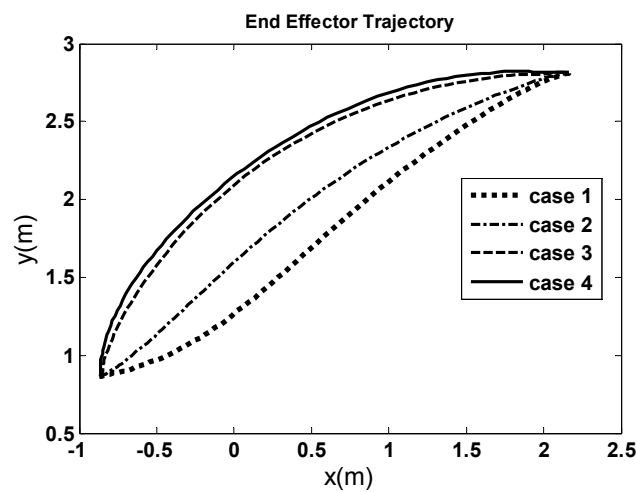Fig. 9. Torques of motors



Fig. 10. Robot Configuration

Fig. 11. End effector trajectory in XY plane

Fig. 8 shows the angular velocities of joints. The computed torques are plotted in Fig. 9. As shown in figures increasing W causes reducing the maximum velocity magnitude while the torques are growing. This issue is predictable, since, in the cost functional defined in the Eq. (16) increasing W causes to rise the role of velocity in path planning an it can decreases the proportion of R in such process. Furthermore, it can be found from figures, in order to attain a smoother path with smaller amount of velocity, more effort must be applied. Also, it is obvious that all the obtained graphs are satisfied the system cost function in Eq. (16). hence, they specify optimal trajectories of the system motion. Therefore, in the proposed method designer is able to choose most appropriate path among various optimal paths according to designing requirements. Robot configuration and end effector trajectory are depected in Figs. 10 and 11 respectively.

3.2.2.2 Motion planning for different payloads

In this case W is assumed to be constant at W=1. Then, the robot path planning problem will be investigated by increasing the payload mass until maximum allowable load will be determined. This maximum payload is obtained as 8.4 kg (case 4). The obtained angular positions, angular velocities and torque curves graphs for a range of $m_P$ given in Table 2 are shown in Fig.s 12 - 14. It can be found that, increasing the $m_P$ results to enlarge the velocity values as a consequence various optimal paths have been attained. As shown in figures, increasing the payload increases the required torque until the maximum payload. So that for the last case the torque curves lay on their limits. Hence, it is the most possible values of the torques and increasing the payload can lead to violate the boundary conditions. Finally, end effector trajectories in the Cartesian space are depicting in Fig. 15.

| Case | 1 | 2 | 3 | 4 |
|------|---|---|---|---|
| $m_p$ | 1 | 3 | 7 | 8.4 |

Table 2. The values of $m_p$ used in the simulation.

$m_{pmax}$ =8.4 kg is the maximum allowable payload for the selected penalty matrices while choosing the other penalty matrices, results in other optimal trajectories. To demonstrate that issue, simulations are carried out for different values of W given in Table 3.
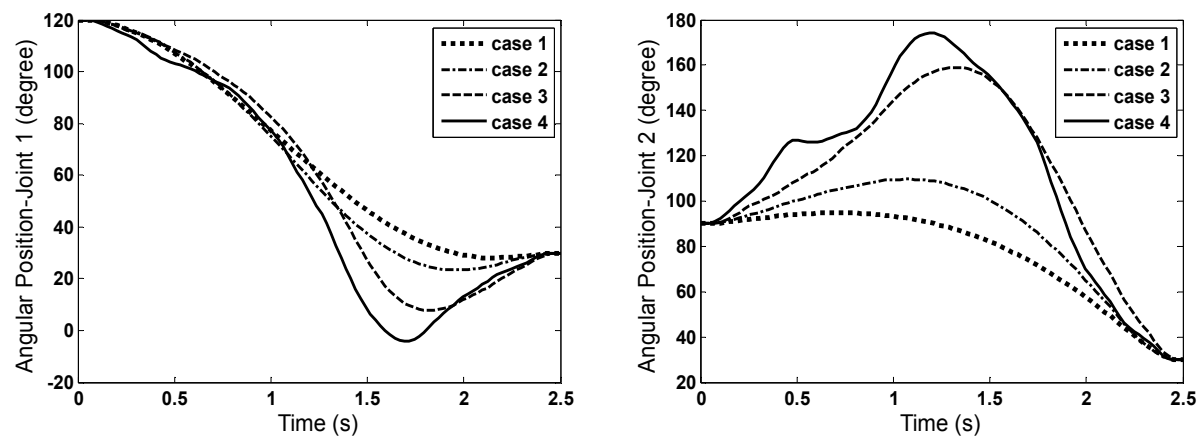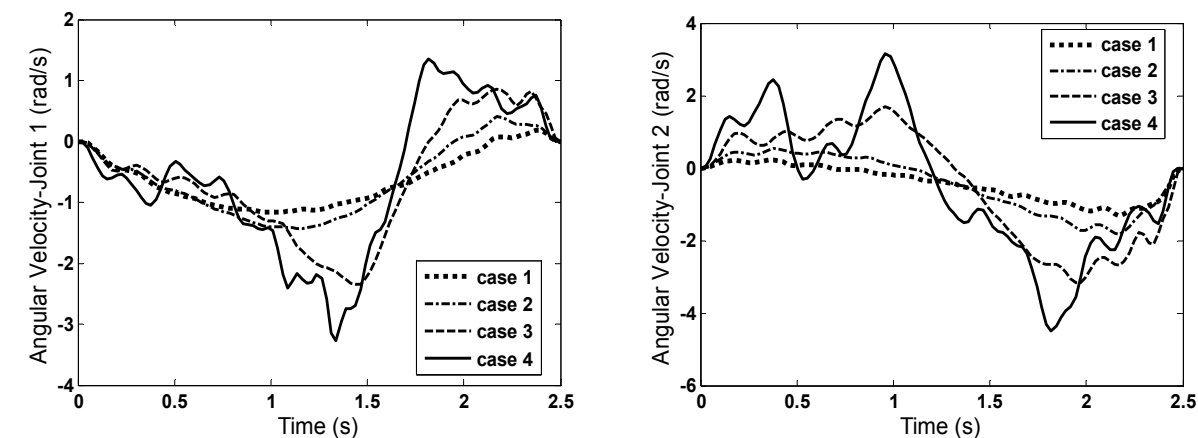
Fig. 12. Angular positions of joints



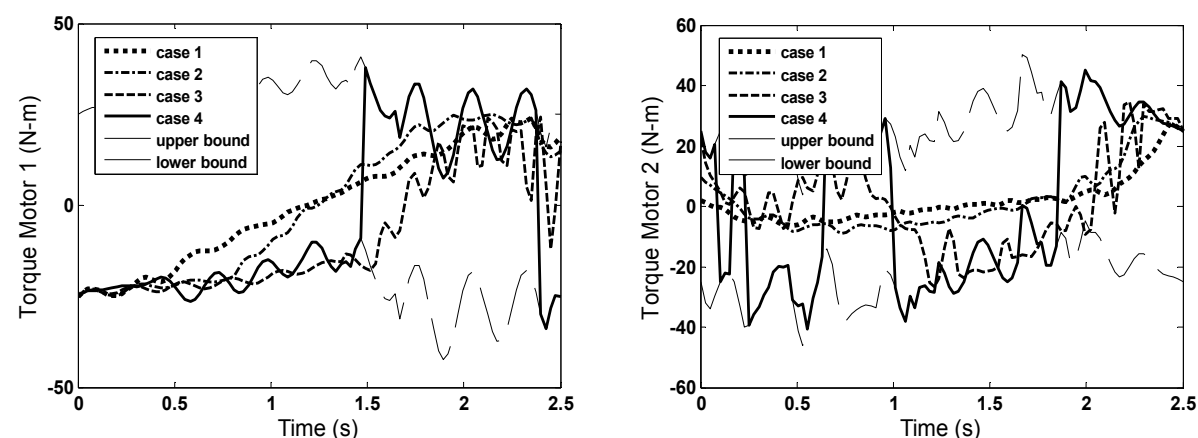Fig. 13. Angular velocities of joints
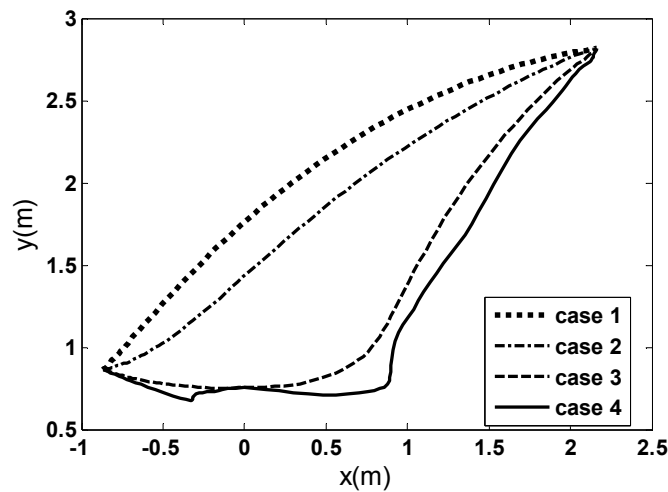


Fig. 14. Torques of motors

Fig. 15. End effector trajectory in XY plane

### 3.2.3 Maximum payload determination
In this case, the maximum payload of flexible mobile manipulator will be calculated and corresponding optimal trajectory at point-to-point motion will be illustrated for different values of W. Payload paths for these cases are shown in Fig. 16. Fig. 17 shows the robot configuration for the first and last cases. Also, he computed torques for these cases are plotted in Fig.18. As it can be seen, increasing W causes to increase oscillatory behavior of the systems that results to reduce the maximum dynamic payload as shown in Table 3.

| Case | 1 | 2 | 3 | 4 |
|---|---|---|---|---|
| W | 1 | 400 | 600 | 800 |
| $m_{p\,max}$ | 8.4 | 7.9 | 7.5 | 6.3 |

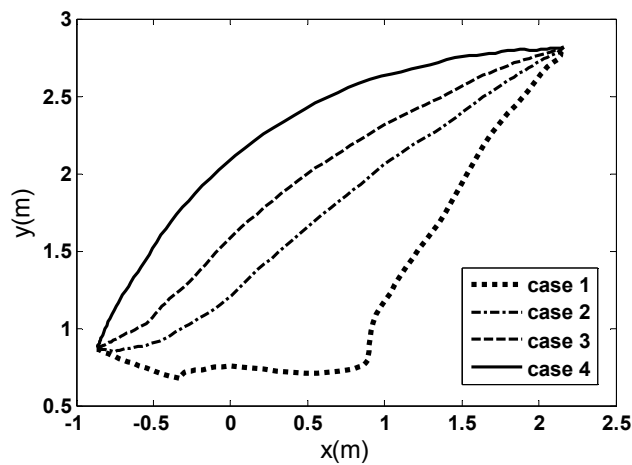Table 3. The values of W and corresponding calculated maximum payloads



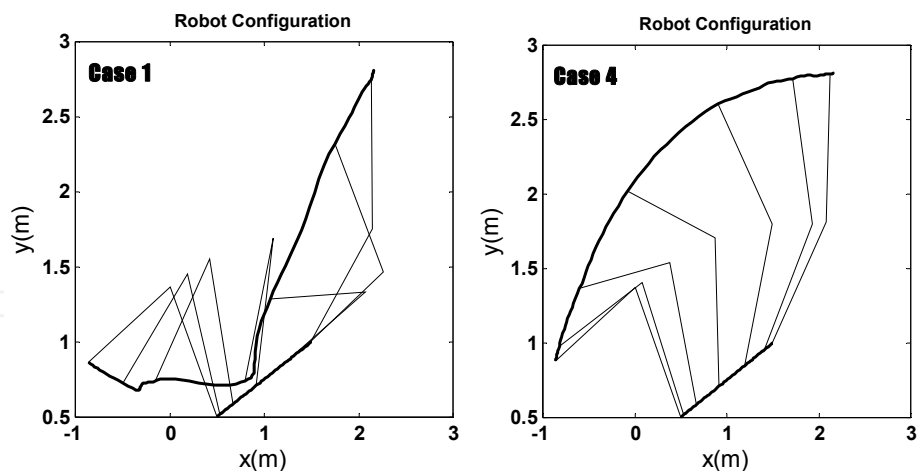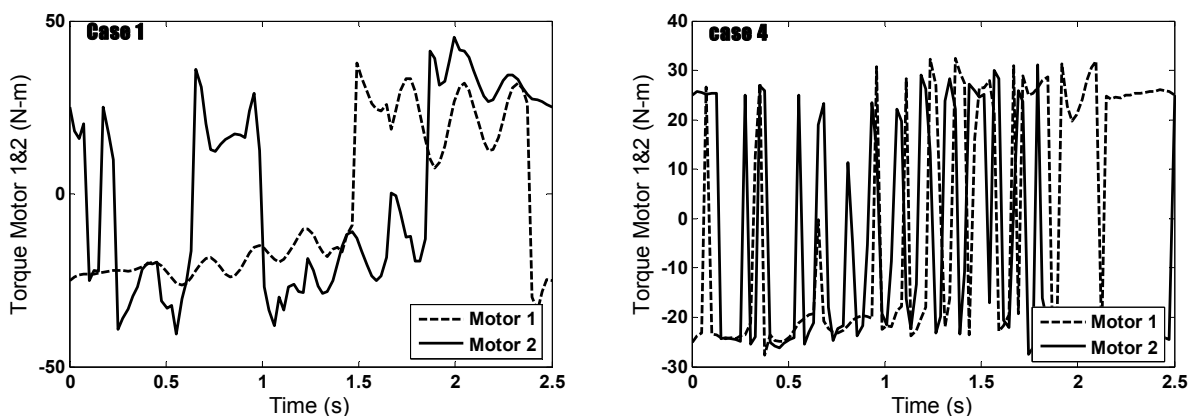Fig. 16. End effector trajectory in XY plane

Fig. 17. Robot Configuration



Fig. 18. Torques of motors

## 4. Conclusion

In this chapter, modelling and control of mechanical manipulator had been studied. First, kinematic and dynamic modelling of flexible link, flexible joint and mobile manipulators have been considered. Then, optimal control of a flexible mobile manipulator in point-to-point motion had been formulated based on the open-loop optimal control approach. The first objective of the chapter is to state the dynamic optimization problem under a quite generalized form in order to be applied to a variety of situations with any guess objective functions for the optimality solution. The second objective is consisting in developing the method for optimizing the applicable case studies, which results.

Using assumed mode and finite element methods oscillatory behavior of he mobile robotic manipulators had been described. The model equations had been verified for a two-link manipulator, and the model responses had been discussed. Then, joint flexibility had been added to the system and obtained model had been simulated. After that, an efficient solution on the basis of TPBVP solution had been proposed to path optimization – maximum payload determination in order to achieve the predefined objective. The solving strategy makes it possible to get any guess objective functions for the optimality solution. Attaining the minimum effort trajectory along with bounding the obtained velocity magnitude had been chosen at the application example. The obtained results illustrate the

power and efficiency of the method to overcome the highly nonlinearity nature of the optimization problem which with other methods, it may be very difficult or impossible. Highlighting the main contribution of the chapter can be presented as:

- The proposed approach can be adapted to any general serial manipulator including both non-redundant and redundant systems with link flexibility and base mobility.
- In this approach the nonholonomic constraints do not appear in TPBVP directly, unlike the method given in (Mohri et al. 2001; Furuno et al. 2003).
- This approach allows completely nonlinear states and control constraints treated without any simplifications.
- The obtained results illustrate the power and efficiency of the method to overcome the high nonlinearity nature of the optimization problem, which with other methods, it may be very difficult or impossible.
- In this method, boundary conditions are satisfied exactly, while the results obtained by methods such as Iterative Linear Programming (ILP) have a considerable error in final time (Ghariblu & Korayem, 2006).
- In this method, designer is able to choose the most appropriate path among various optimal paths by considering the proper penalty matrices.

The optimal trajectory and corresponding input control obtained using this method can be used as a reference signal and feed forward command in the closed-loop control of such manipulators.

## 5. References

Bertolazzi E.; Biral F. & Da Lio M. (2005). Symbolic–numeric indirect method for solving optimal control problems for large multibody systems, *Multibody System Dynamics*, Vol. 13, No. 2, pp. 233-252

Bessonnet G. & Chessé S. (2005). Optimal dynamics of actuated kinematic chains, Part 2: Problem statements and computational aspects, *European J. of Mechanics A/Solids*, Vol. 24, pp. 472–490

Bloch A. M. (2003). Nonholonomic mechanics and control. *Springer,* New York

Bock H. G. & Plitt K. J. (1984). A multiple shooting algorithm for direct solution of optimal control problems, *Proc. 9th IFAC World Congress*, pp. 242–247

Callies R. & Rentrop P. (2008). Optimal control of rigid-link manipulators by indirect methods, *GAMM-Mitt.*, Vol 31, No. 1, pp. 27 – 58

Chen W. (2001). Dynamic modelling of multi-link flexible robotic manipulators, *Computers and Structures*, Vol. 79, (2), pp. 183–195

Furuno S.; Yamamoto M. & Mohri A. (2003). Trajectory planning of mobile manipulator with stability considerations, *Proc. IEEE Int. Conf. on Robotics and Automation*, pp. 3403-3408

Ghariblu H. & Korayem M. H. (2006). Trajectory Optimization of Flexible Mobile Manipulators, *Robotica*, Vol. 24, No. 3, pp. 333-335

Green A. & Sasiadek J.Z. (2004). Dynamics and Trajectory Tracking Control of a Two-Link Robot Manipulator, *Journal of Vibration and Control*, Vol. 10, No. 10, pp. 1415–1440

Hargraves C. R. & Paris S. W. (1987). Direct trajectory optimization using nonlinear programming and collocation, *AIAA J. Guidance*, Vol. 10, No. 4, pp. 338–342, 1987.

Korayem M. H. & Ghariblu H. (2004). Analysis of wheeled mobile flexible manipulator dynamic motions with maximum load carrying capacities, *Robotics and Autonomous Systems*, Vol. 48, No. 2-3, pp. 63-76

Korayem M.H. & Rahimi Nohooji H. (2008). Trajectory optimization of flexible mobile manipulators using open-loop optimal control method, *LNAI*, Springer-Verlag Berlin Heidelberg, Vol. 5314, Part 1, pp. 54–63.

Korayem M. H.; Haghpanahi M. ; Rahimi H. N. & Nikoobin A. (2009). Finite element method and optimal control theory for path planning of elastic manipulators, *New Advanced in Intelligent Decision Technology., SCI,* Springer-Verlag Berlin Heidelberg, Vol. 199, pp. 107-116

Korayem M. H.; Rahimi H. N. & Nikoobin A.  (2009). Analysis of Four Wheeled Flexible Joint Robotic Arms with Application on Optimal Motion Design, *New Advanced in Intelligent Decision Technology., SCI,* Springer-Verlag Berlin Heidelberg, Vol. 199, pp. 117-126

Mohamed Z. & Tokhi M.O. (2004). Command shaping techniques for vibration control of a flexible robot manipulator, *Mechatronics*, Vol. 14, pp. 69–90.

Mohri A.; Furuno S. & Yamamoto M. (2001). Trajectory planning of mobile manipulator with end-effector's specified path, *Proc. IEEE Int. Conf. on Intelligent Robots and systems*, pp. 2264-2269

Papadopoulos E. & Rey, D. (1996). A New measure of tip over stability margin for mobile manipulators, *Proc. IEEE Int. Conference on Robotics and Automation*, pp. 3111-3116

Papadopoulos E. & Gonthier, Y. (1999) A framework for large-force task planning of mobile redundant manipulators, *J. of Robotic Systems*, Vol. 16, No. 3, pp. 151-162

Papadopoulos E.; Poulakakis I. & Papadimitriou I. (2002). On path planning and obstacle avoidance for nonholonomic platforms with manipulators: *A polynomial approach, Int. J. of Robotics Research*, Vol. 21, No. 4, pp. 367-383

Rahimi H. N.; Korayem M. H.  & Nikoobin A. (2009). Optimal Motion Planning of Manipulators with Elastic Links and Joints in Generalized Point-to-Point Task, *ASME International Design Engineering Technical Conferences & Computers and Information in Engineering Conference (IDETC/CIE)*, Vol. 7, *Part B, 33rd Mechanisms and Robotics Conference*, pp 1167-1174, San Diego, CA, USA

Sentinella M. R. & Casalino L. (2006). Genetic algorithm and indirect method coupling for low-thrust trajectory optimization, *42nd AIAA/ASME/SAE/ASEE Joint Propulsion Conference and Exhibit*, California

Seraji H., "A unified approach to motion control of mobile manipulators, *Int. J. of Robotic Research*, Vol. 17, No. 12, pp.107–118 (1998).

Shampine L. F.; Reichelt M. W. & Kierzenka J. Solving boundary value problems for ordinary differential equations in MATLAB with bvp4c, available at http://www.mathworks.com/bvp tutorial

Sheng Ge Xin & Qun Chen Li. (2006). Optimal motion planning for nonholonomic systems using genetic algorithm with wavelet approximation, *Applied Mathematics and Computation*, Vol. 180, pp. 76–85

Subudhi B. & Morris A.S. (2002). Dynamic Modelling, Simulation and Control of a Manipulator with Flexible Links and Joints, *Robotics and Autonomous Systems*, Vol. 41, pp. 257–270

Usoro P.B.; Nadira R., Mahil S. S. (1986). A finite element/Lagrange approach to modelling lightweight flexible manipulators, *J. of Dynamics Systems, Measurement*, and Control, Vol. 108, pp.198–205

Wachter A. & Biegler L. T. (2006). On the implementation of an interior-point filter line-search algorithm for large-scale nonlinear programming, *Mathematical Programming*, Vol. 106, No. 1, pp. 25–57

Yue S., Tso S. K. & Xu W. L. (2001).  Maximum dynamic payload trajectory for flexible robot manipulators with kinematic redundancy, *Mechanism and Machine Theory* 36, 785–800

Zhang C. X. & Yu Y. Q. (2004). Dynamic analysis of planar cooperative manipulators with link flexibility, *ASME Journal of Dynamic Systems, Measurement, and Control,* Vol. 126, pp. 442–448
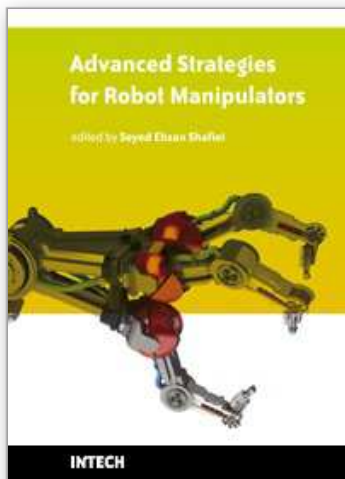
**Advanced Strategies for Robot Manipulators**

Edited by S. Ehsan Shafiei

ISBN 978-953-307-099-5

Hard cover, 428 pages

**Publisher** Sciyo

**Published online** 12, August, 2010

**Published in print edition** August, 2010

Amongst the robotic systems, robot manipulators have proven themselves to be of increasing importance and are widely adopted to substitute for human in repetitive and/or hazardous tasks. Modern manipulators are designed complicatedly and need to do more precise, crucial and critical tasks. So, the simple traditional control methods cannot be efficient, and advanced control strategies with considering special constraints are needed to establish. In spite of the fact that groundbreaking researches have been carried out in this realm until now, there are still many novel aspects which have to be explored.

**How to reference**

In order to correctly reference this scholarly work, feel free to copy and paste the following:

Hamed Rahimi Nohooji (2010). The Comparative Assessment of Modeling and Control of Mechanical Robot Manipulators, Advanced Strategies for Robot Manipulators, S. Ehsan Shafiei (Ed.), ISBN: 978-953-307-099-5, InTech, Available from: http://www.intechopen.com/books/advanced-strategies-for-robot-manipulators/-the-comparative-assessment-of-modeling-and-control-of-mechanical-robot-manipulators-

# INTECH
open science | open minds